

Planetary Nebulae in the eROSITA eRASS1 catalog

HAOYANG YUAN,^{1,2} MARTIN A. GUERRERO,³ QUENTIN PARKER¹ AND RODOLFO MONTEZ JR.⁴
THE HKU-IAA PN COLLABORATION

¹*Laboratory for Space Research, The University of Hong Kong, Hong Kong*

²*Department of Physics, The University of Hong Kong, Hong Kong*

³*Instituto de Astrofísica de Andalucía, IAA-CSIC, Glorieta de la Astronomía S/N, Granada E-1800, Spain*

⁴*Center for Astrophysics | Harvard & Smithsonian, Cambridge, MA, USA*

ABSTRACT

Some planetary nebulae (PNe) host X-ray-emitting hot bubbles shaped by stellar wind interactions and/or harbor X-ray-emitting central stars due to accretion, shocks within their fast stellar winds, or even chromospheric emission from binary companions. In both cases, the properties of the X-ray emission critically probe late-stages of stellar evolution for such low- and intermediate-mass stars. While extant Chandra and XMM-Newton observations have detected X-ray emission in PNe, the numbers known remain very small (~ 40) compared to the overall Galactic PNe population (~ 4000). We have initiated a project aimed at increasing the sample of known PNe with X-ray emission using both current and new space-based X-ray telescopes such as the Einstein probe. To further investigate their X-ray properties to elucidate what drives current X-ray PN detections, we have cross-searched the SRG *eROSITA-DE* eRASS1 source catalogue and Hong Kong (HASH) PNe Database. Five known X-ray PNe have been detected (Abell 30, NGC 2392, NGC 3242, NGC 5315, and LoTr 5), two new X-ray PNe are revealed (IC 1297 and NGC 2867), one (K 1-27) is removed from previous X-ray compilations, and another 11 previously detected X-ray emitting PNe are not recovered. A comparison of the X-ray flux of detected and undetected X-ray PNe reveals that eROSITA eRASS1 is sensitive to PNe with X-ray fluxes larger than $\approx 2 \times 10^{-14}$ erg cm⁻² s⁻¹. The frequency of occurrence is $\simeq 0.5\%$ among the 1430 HASH True PNe in the eRASS1 footprint.

Keywords: High Energy astrophysics (739) — Interstellar medium (847) — Stellar astronomy (1583)
— Planetary Nebulae (1249)

1. A SHORT HISTORY OF PLANETARY NEBULAE WITH X-RAY EMISSION

Planetary nebulae (PNe) are a short-lived phase in the late evolutionary stages of low- and intermediate-mass stars. Since the first detection of X-ray emission from NGC 1360 by EXOSAT (P. A. J. de Korte et al. 1985), more than 40 years ago, PNe have been selectively targeted by any available X-ray mission (e.g., ROSAT, M. A. Guerrero et al. 2000). This has steadily but only gradually increased their number until the ambitious *Chandra Planetary Nebulae Survey* (ChanPlaNS) large programs targeted a large fraction of all PNe closer than 1.5 kpc. This resulted in a major increase in the number of X-ray PNe up to $\simeq 40$ (J. H. Kastner et al. 2012; M. Freeman et al. 2014; R. Montez et al. 2015). This has led to unprecedented progress in the understanding of the nature of X-ray sources in PNe.

PNe can exhibit point and extended sources of X-rays. The former are associated with their central stars (CSPNe). Soft X-ray emission ≤ 0.3 keV, originates from photospheric emission from hot stellar photospheres. However, there are many cases when their X-ray emission is harder, ≥ 0.5 keV. In those cases, the X-ray emission can be attributed to shocks in winds, as in OB stars (L. B. Lucy & R. L. White 1980), but also to companions, either to the chromospheric emission from a late-type companion (as in the case of LoTr 5, R. Montez et al. 2010) or to accretion onto the CSPN (as can be the case of NGC 2392, M. A. Guerrero et al. 2019).

The observed diffuse X-ray emission can actually be expected in the framework of the interacting stellar winds model (ISW) of PN formation (S. Kwok et al. 1978). The interaction of the dense and slow stellar wind ejected during the asymptotic giant branch (AGB) phase with the strong fast stellar wind from the CSPN produces a reverse shock heating the stellar wind to X-ray-emitting temperatures $\approx 10^7$ K as in wind-blown bubbles (R. Weaver et al. 1977). Heat-conduction, photo-evaporation, and turbulent mixing are expected to increase the density and emissivity of the X-ray emitting material while lowering its temperature down to several 10^6 K (J. A. Toalá & S. J. Arthur 2016). The diffuse X-ray emission from these hot bubbles is thus soft and enclosed in most cases by sharp inner rims of some young, compact and dense PNe.

Chandra and XMM-Newton have produced, for the first time, decent X-ray images and spectra of PNe. However, targeted observations have only been obtained for a very limited sample out of the 3957 known True (2787), Likely (459), and Possible (711) Galactic PNe, as recorded in the HASH PNe database (Q. A. Parker et al. 2016a). Moreover, their X-ray observations have been biased towards high surface brightness and well-studied PNe to increase the chances of detection and their value to broad, multi-wavelength comparisons of these often well studied PNe. X-ray all-sky surveys, on the other hand, can probe the whole sample of Galactic PNe to assess the effects of distance, extinction, binarity, extant physical processes, and evolutionary state on the X-ray detectability and X-ray properties of all PNe. Previously this was only available for the low-resolution ROSAT All-Sky Survey (RASS), with a lower flux limit of a few times 10^{-13} erg cm $^{-2}$ s $^{-1}$ (T. Boller et al. 2016) compared to more recent X-ray telescopes like Chandra and XMM-Newton. ROSAT data are both limited and too shallow to allow this investigation. However, the partial release of the *eROSITA* all-sky survey (the *eROSITA-DE* eRASS1, P. Predehl et al. 2021), with an increase in sensitivity of at least a factor of 10 over the ROSAT all-sky survey, provides a unique opportunity to search for new X-ray-emitting PNe and to derive global properties for their X-ray emission.

We present here a search for new X-ray PNe using the *eROSITA-DE* eRASS1 source catalog. The cross-correlation between the known population of Galactic PNe and the sky footprint covered by *eROSITA-DE* eRASS1 is described in §2. The results of this search is presented in §3 and the implications for overall X-ray properties of PNe are discussed in §4. The conclusions and expectations for new X-ray missions, as the Einstein Probe, are laid out in §5.

2. THE SAMPLE OF PLANETARY NEBULAE AND THE EROSITA ERASS1 CATALOG

2.1. The HASH Database: The comparison sample of Galactic PNe

For comparison purposes with the X-ray data, this study uses the best available PNe optical images and spectroscopy from the Hong Kong/Australian Astronomical Observatory/Strasbourg Observatory H-alpha Planetary Nebula research platform database (HASH, see Q. A. Parker et al. 2016a). This is further supplemented by new, very deep, narrow-band imaging from Peter Goodhew⁵, one of our amateur collaborators that are now regularly providing the best such PNe images currently available (e.g., P. Le Dû et al. 2022). HASH contains the consolidated discoveries and data for all known Galactic PNe in terms of multi-wavelength imagery, spectroscopy and other key parameters (angular size, morphology, central star identifications, and more) from compiling over 200 years of cataloguing and PNe discovery work in the field. PNe central coordinates are derived from a fit to the overall geometric shape of the PNe, independent of any putative CSPN. For the vast majority of PNe, this is straightforward. Such PNe geometric centroid positions are usually very close to the position of well-identified CSPNe. In a few cases, there is a modest (few arcseconds) offset, sometimes seen in asymmetrically shaped PNe that may be interacting with the ISM. For further details see Q. A. Parker et al. (2006), Q. A. Parker et al. (2016b) and Q. A. Parker (2022).

2.2. The *eRosita* and *eRASS1* X-ray source catalogue of the Western Galactic Hemisphere ($l \gtrsim 180^\circ$)

eROSITA (the extended Roentgen Survey with an Imaging Telescope Array) is an array of seven Wolter-I X-ray telescope modules, each equipped with 54 mirror shells and with an outer diameter of 36 cm on board the Russian-German Spektrum Roentgen Gamma (SRG) spacecraft. With a field of view of 1.03 degrees, it provides a wide field survey capability with high-throughput X-ray spectroscopic imaging in the 0.2-8 keV energy range with energy resolution $\simeq 80$ eV at 1.5 keV (P. Predehl et al. 2021). Launched on 2019 July 13, its main goal is conducting a comprehensive X-ray survey of the entire sky, concluding its initial 184-day all-sky survey on 2020 June 11. Although primarily intended to map dark matter and Galaxy clusters, it has proven useful for any astrophysical source that emits sufficient X-ray flux to fall above the survey sensitivity limits. *eRosita* has a nominal all-sky flux sensitivity

⁵ <https://www.imagingdeepspace.com/peter-goodhew-planetary-nebulae-images.html>

Table 1. X-ray-emitting true Galactic PNe now also detected in the eROSITA-DE eRASS1 catalog.

PNG Name	HASH #	Common Name	eRASS1 IAU name (J2000 RA/DEC)	Offset (arcsec)	Position 1- σ (arcsec)	Nebular diameter (arcsec)	Median energy (KeV)	Count number	Count Rate (s ⁻¹)
PNG 197.8+17.3	730	NGC 2392	1eRASS J072910.7+205444	2.4	4.9	46	0.48	7.1 \pm 2.8	0.094 \pm 0.038
PNG 208.5+33.2	742	Abell 30	1eRASS J084653.3+175248	3.0	6.5	127	0.40	5.2 \pm 2.6	0.071 \pm 0.036
PNG 261.0+32.0	824	NGC 3242	1eRASS J102446.3-183822	10.8	4.1	32	0.46	6.2 \pm 2.7	0.083 \pm 0.036
PNG 309.1-04.3	955	NGC 5315	1eRASS J135357.4-663046	5.4	2.0	11	0.62	43.2 \pm 7.1	0.264 \pm 0.043
PNG 339.9+88.4	1082	LoTr 5	1eRASS J125533.9+255339	9.0	3.6	525	0.73	17.9 \pm 4.7	0.136 \pm 0.035

limit of 5×10^{-14} erg cm⁻² s⁻¹ that improves at high ecliptic latitudes due to the all-sky survey scanning pattern. Unlike Chandra and XMM-Newton, intended as X-ray observatories targeting specific sources, eRosita provides not just Galactic plane coverage but all sky survey capabilities and so greater source discovery opportunities at the relevant sensitivities available.

The first data release of the Western⁶ Galactic hemisphere of the *eROSITA* all-sky survey (the *eROSITA-DE* eRASS1, hereafter eRASS1) was made public on 2024 January 31 (A. Merloni et al. 2024). eRASS1 provides calibrated data products and source catalogs processed using the *eROSITA* standard pipeline. Here we will use the eRASS1 Main catalog, with calibrated event files and count numbers, count rates, flux estimates, detection likelihood, observing time, and quality flags for 903521 point sources and 26682 extended sources detected in the 0.2-2.3 keV band. The survey is also sensitive in the harder X-ray range of 2.3-5 keV.

2.3. Cross-correlation of the Planetary Nebulae sample with the eRASS1 catalog

We cross correlated the positional information for all true (T), likely (L) and possibly (P) Galactic PNe in HASH with sources in the eRASS1 Main catalog. Considering the typical soft X-ray emission exhibited by PNe, the main catalogue used is that for the soft 0.2-2.3 keV *eROSITA* ML1 band. Given the typical eRASS1 imaging resolution (HEW \approx 30'') and the possible crowding at the location of some PNe in the Galactic Plane, the search was initially limited to X-ray sources with a positional coincidence within 20'' of a HASH Galactic PN. This resulted in the 10 eRASS1 PN candidates listed in Tables 1, 2, and 3. The results are presented below. If we relax this conservative limit to 45'' a further 7 potential matches to known Galactic PNe were uncovered. On examination none of these are plausible matches. Six of the PNe were compact with no overlap and clear separation between the outermost contours derived from the low X-ray source counts and the PNe. One PN Abell 26 is well resolved with an angular size of 38 arcsec. Here, the outermost X-ray contours impinge on the western edge of the PNe while the centre of the PNe and X-ray source are offset by \sim 30-arcseconds. This is a poor match compared to all others plausible matches we have presented and is discounted here.

3. RESULTS

The quality of the association between these 10 PNe and their possible X-ray counterparts in the eRASS1 main source catalogue was then individually assessed. *eROSITA* 0.2-2.0 keV X-ray images of these eRASS1 PN candidates were extracted from the event files and then compared to their optical images to make this assessment (Figs. 1, 2 and 3). We present 3 images for each X-ray candidate per row. The leftmost panels show the *eROSITA* X-ray photon detections. The pixel size of these images has been binned to 10 arcsec to properly sample the \simeq 30 arcsec spatial resolution of *eROSITA*. The images are additionally overlaid with X-ray contours derived from images smoothed using a Gaussian profile with a 2-pixel kernel. The images cover an area of 7 \times 7 arcminutes in and around the PN to show the X-ray detection in better context with the background, given the low count rates typical for all X-ray sources. In the middle panels we show, at the same angular size, the grey-scale, optical, narrow-band B-band image of the PNe taken from the SuperCOSMOS sky survey (Q. A. Parker et al. 2005) for all southern objects and JPLUS (A. J. Cenarro et al. 2019) for the Northern hemisphere objects so that the positional coincidence can be discerned. These images are overlaid with the same X-ray contours. Finally, as it is hard to see any structural detail in the optical PN images, given their generally small angular size and high surface brightness in the larger area 7 \times 7 arcminutes images, we provide in the rightmost panels zoomed in colour, combined narrow-band images of each PNe from the best available sources,

⁶ Data rights are split by Galactic longitude (l) and latitude (b). Data with $-0.05576432^\circ < l < 179.94423568^\circ$ (Eastern Galactic hemisphere) belong to the Russian consortium, while data with $179.94423568^\circ < l < 359.94423568^\circ$ (Western Galactic hemisphere) belong to the German consortium and are the only ones currently available and provided by eROSITA-DE.

Table 2. Two true Galactic PNe with new X-ray detections in the *eROSITA*-DE eRASS1 catalog.

PNG Name	HASH #	Common Name	eRASS1 IAU name (J2000 RA/DEC)	Offset (arcsec)	Position 1- σ (arcsec)	Nebular diameter (arcsec)	Median energy (KeV)	Count number	Count Rate (s^{-1})
PNG 278.1–05.9	858	NGC 2867	1eRASS J092125.6–581843	3.6	3.6	14.4	0.55	8.7 ± 3.3	0.032 ± 0.012
PNG 358.3–21.6	1267	IC 1297	1eRASS J191723.2–393639	6.6	3.7	10.8	0.44	7.3 ± 4.0	0.091 ± 0.038

Table 3. Three true Galactic PN with spurious X-ray counterparts in the *eROSITA*-DE eRASS1 catalog.

PNG Name	HASH #	Common Name	eRASS1 IAU name (J2000 RA/DEC)	Offset (arcsec)	Position 1- σ (arcsec)	Nebular diameter (arcsec)	Median energy (KeV)	Count number	Count Rate (s^{-1})
PNG 286.8–29.5	888	K 1-27	1eRASS J055657.9–754015	17.4	3.7	61	12.5 ± 4.8	0.021 ± 0.008	1.01
PNG 351.7–10.9	1157	Wray 16-385	1eRASS J181254.3–413029	16.2	2.7	8	15.4 ± 4.3	0.182 ± 0.501	0.65
PNG 289.0–03.3	2672	PHR J1107–5642	1eRASS J110744.1–564240	16.2	5.6	188	8.4 ± 3.8	0.035 ± 0.015	0.91

including from HST and deep amateur imagery from Peter Goodhew . The interesting morphological structures and CSPN detections can now be properly appreciated in Figs. 1, 2 and 3.

After inspecting those images, any PN with a positional coincidence between the HASH and the eRASS1 counterpart, accounting both for the eRASS1 positional uncertainty and the PN angular extent, and with a count rate at least twice the count rate uncertainty were considered bona-fide X-ray PNe in the *eROSITA* eRASS1 catalogue. These include five PNe already known to be X-ray-emitters (Tab. 1, Fig. 1) and another two newly identified X-ray emitting PNe, IC 1297 and NGC 2867 (Tab. 2, Fig. 2). Another three not fulfilling the above criteria or resulting in unconvincing matches after the examination of their optical and X-ray images were found. This includes K 1-27 that was previously identified as a PN exhibiting X-ray emission (T. Rauch et al. 1994a). The two other potential X-ray emitting PNe considered unlikely X-ray PNe in the *eROSITA* eRASS1 catalogue after vetting here (Tab. 3, Fig. 3), are Wray 16-385, and PHR J1107–5642. The *eROSITA* background-subtracted X-ray spectra of these PNe are presented in Figs. 4 and 5.

A short description of the PNe and the spatial and spectral properties of their associated X-ray emission uncovered by this cross-matching process is provided below for each case referred to above. This includes PNe previously known to have X-ray detections and new candidates uncovered by this work, as well as the deduced spurious eRASS1 counterparts of PNe.

3.1. Known X-ray Galactic PNe with *eROSITA* eRASS1 counterparts

In this section, we examine the known X-ray emitting PNe that fall within the currently accessible survey footprint of *eROSITA*.

3.1.1. NGC 2392, the Eskimo Nebula

NGC 2392 is the famous Eskimo Nebula, with a double-shell morphology in the optical. It has been imaged on multiple occasions and with a significant associated literature, e.g. (e.g., F. Gieseking et al. 1985; M. A. Guerrero et al. 2005; M. T. García-Díaz et al. 2012). Its X-ray emission was only tentatively detected in the ROSAT PSPC observations (M. Guerrero et al. 2000) with a count rate of $0.0021 \pm 0.0013 s^{-1}$. The diffuse X-ray emission is confined within its innermost shell as confirmed by XMM-Newton (M. A. Guerrero et al. 2005). The diffuse X-ray emission from NGC 2392 can be described by a hot plasma with a temperature $\simeq 2 \times 10^6 K$ and an X-ray flux in the 0.2–2.5 keV energy range of $(6 \pm 1) \times 10^{-14} \text{ erg cm}^{-2} s^{-1}$. At the Gaia distance of $1830 \pm 90 \text{ pc}$ for its CSPN, the intrinsic X-ray luminosity would be $(4.1 \pm 1.6) \times 10^{31} \text{ erg s}^{-1}$. The spatial distribution of the X-ray emission in the 0.2–0.65 keV band was suggested to align along the fast collimated outflow, but Chandra X-ray observations at much improved spatial resolution do not confirm it. Instead, it revealed the presence of a point-source of hard, up to 3 keV X-ray emission at the central star position of NGC 2392, see (see N. Ruiz et al. 2013; J. H. Kastner et al. 2012). Once the emission from this source is excised, the X-ray flux and intrinsic luminosity are found to be $3.9 \times 10^{-14} \text{ erg cm}^{-2} s^{-1}$ and $2.6 \times 10^{31} \text{ erg s}^{-1}$, respectively. The peculiar, hard X-ray emission of its CSPN is attributed to local scale accretion from a companion, whereas the origin of the diffuse X-ray emission is enigmatic, as the CSPN wind cannot provide the mechanical energy that the observed plasma temperature and luminosity require (M. A. Guerrero et al.

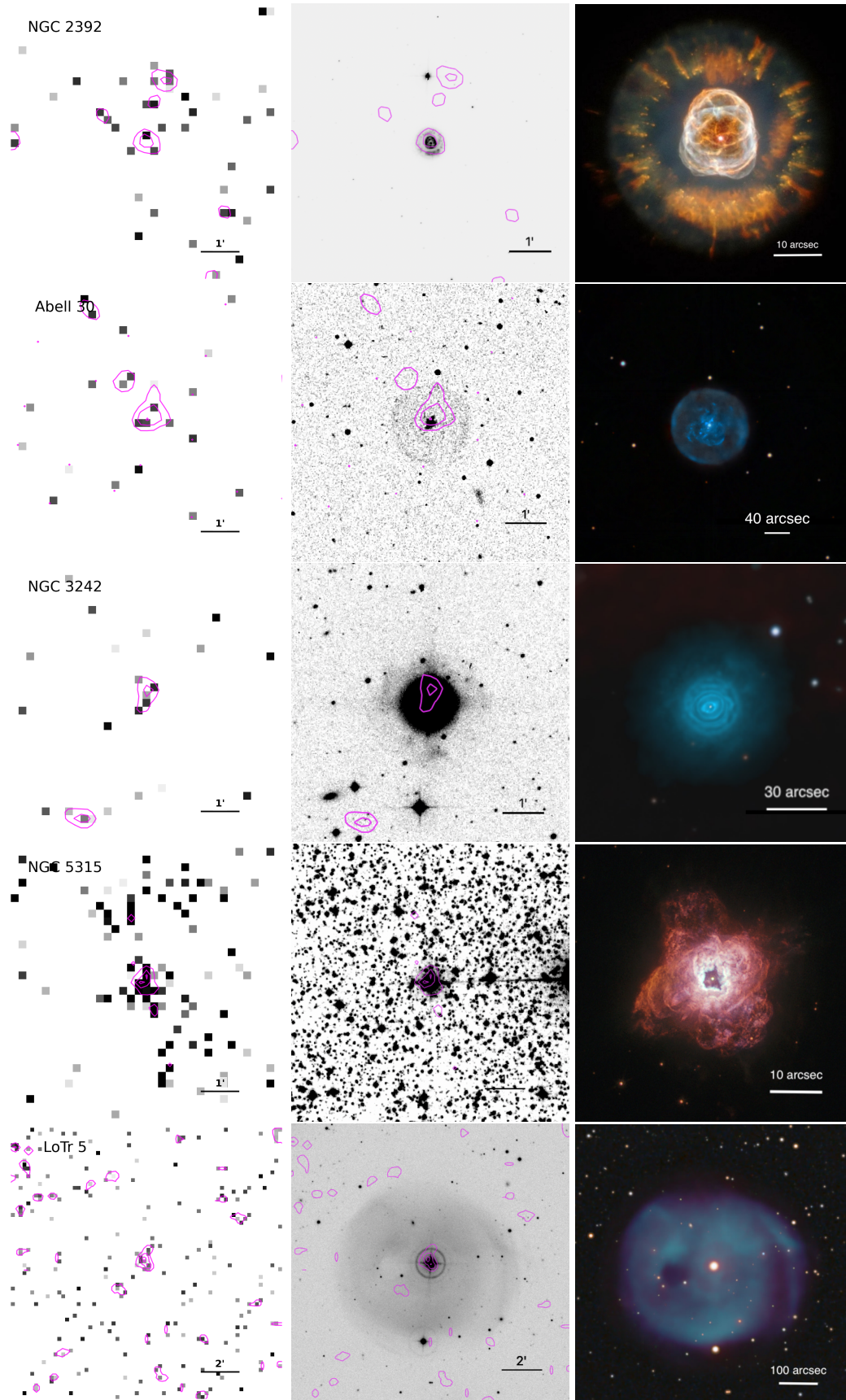


Figure 1. *eROSITA* (left), B-band (middle) and colour-composite optical (right) images of the five already known X-ray PNe. The X-ray and photographic B-band images (left and middle panels) have a similar 7×7 arcmin field of view (LoTr 5 has 14×14 arcmin) and are overlaid by X-ray contours. NGC 2392 and LoTr 5's optical images are from J-PLUS. North is up, east to the left. The final colour image is also NE to top left but is zoomed in to provide the PNe morphological detail, except for LoTr 5, which is already well resolved. The first and 4th colour images are from the HST (image credit NASA/HST), while the 4 other blue dominated images are from the very deep amateur narrow-band [OIII] dominated imagery of Peter Goodhew: <https://www.imagingdeepspace.com/>

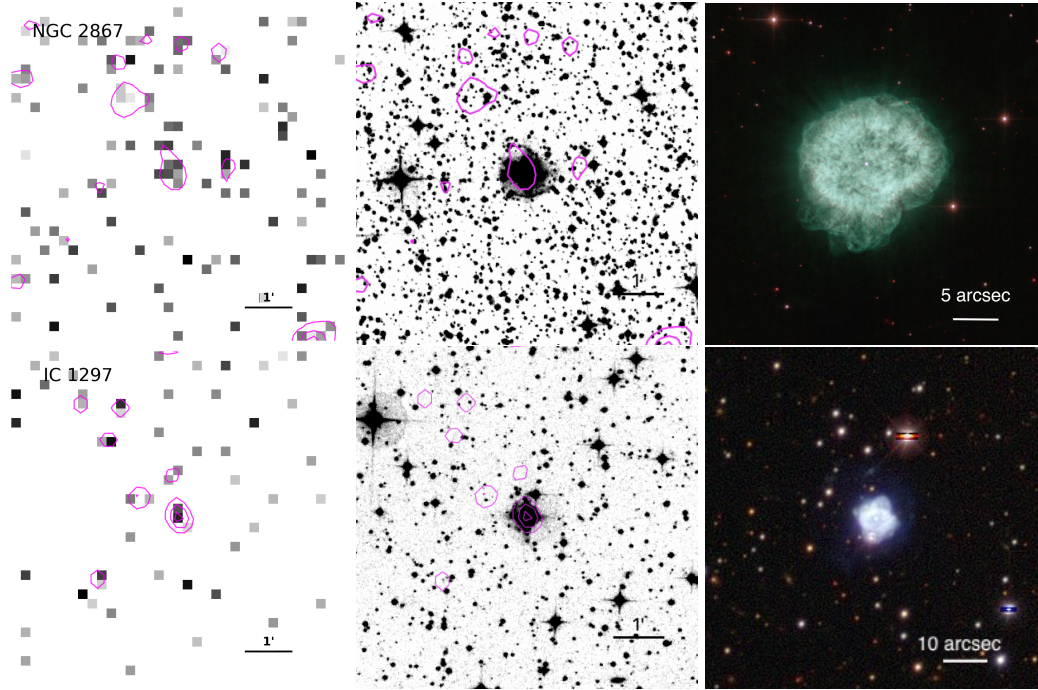


Figure 2. Same as Fig. 1 for the two new X-ray PNe uncovered in eRASS1, with NGC 2867 top and IC 1297 bottom. The colour image for NGC 2867 is from the HST (image credit NASA/HST) while that for IC 1297 is from Legacy Surveys/D. Lang (Perimeter Institute) Filters: g, r, z.

2019; B. Miszalski et al. 2019). Furthermore, the diffuse emission is confined within a hot “floculent” bubble which appears to be a strong morphological trait for all other Galactic PNe with diffuse X-ray emission. A single-lined spectroscopic binary with 1.9-day period in NGC 2392 was confirmed by (B. Miszalski et al. 2019) from a careful, ECHELLE spectrograph-based, radial velocity study of the CSPN.

The X-ray emission detected by *eROSITA* perfectly matches the position of NGC 2392, with most X-ray photons enclosed within the overall inner nebular shell. The low count number, $\simeq 7$, is insufficient for spectral analyses (Fig. 4). The median energy of these events is 0.482 keV, peaking below 0.5 keV. The location of NGC 2392 on Fig. 6 implies spectral properties indicative of a plasma with temperature of $(1 - 2) \times 10^6$ K, which is consistent with the diffuse emission source of NGC 2392 detected by XMM-Newton and Chandra.

3.1.2. Abell 30

Abell 30 is another very unusual, so-called “born again” PN (e.g. G. H. Jacoby & H. C. Ford 1983; R. Wesson et al. 2005) with a high abundance discrepancy factor shown by R. Wesson et al. (2018) to be a strong indicator of CSPN binarity and recently confirmed as such (G. H. Jacoby et al. 2020). ROSAT first detected diffuse X-ray emission with plasma temperatures of $(2 - 4.5) \times 10^5$ K, fitted by an optically-thin plasma emission model. The X-ray emission is very soft, with almost all source counts at energies below 0.4 keV (Y.-H. Chu & C.-H. Ho 1995). The comparison with HST WFPC2 imagery of this PN revealed the significant spatial correspondence between the X-ray and optical emission centroids for both a bipolar pair of knots and a clumpy, expanding disk (Y. Chu et al. 1997). The diffuse X-ray emission of Abell 30 has been suggested to be generated by the fast stellar wind interactions with the hydrogen-poor ejecta of the reborn process, either by stellar wind ablation in high electron density environments ($\sim 1000 \text{ cm}^{-3}$) or by charge-exchange reactions with neutral material (M. A. Guerrero et al. 2012). Analyses of XMM-Newton and Chandra spectra imply a plasma temperature of 0.79×10^6 K. The observed flux in $0.2 - 1.5$ keV energy range is $(2.8 \pm 0.9) \times 10^{-14} \text{ erg cm}^{-2} \text{ s}^{-1}$, and the intrinsic luminosity at the Gaia distance of $2210 \pm 160 \text{ pc}$ is $\sim 1.3 \times 10^{31} \text{ erg s}^{-1}$.

The X-ray emission detected by *eROSITA* perfectly matches the position of Abell 30, with most X-ray photons around the central star and H-deficient knots. The low X-ray photon count number, $\simeq 5$, is again insufficient for spectral analyses. Their median energy is 0.40 keV and their X-ray spectrum is soft, peaking below 0.5 keV (Fig. 4). The temperature implied by a typical plasma emission model is low, $\simeq 1 \times 10^6$ K (Fig. 6), but higher than that derived

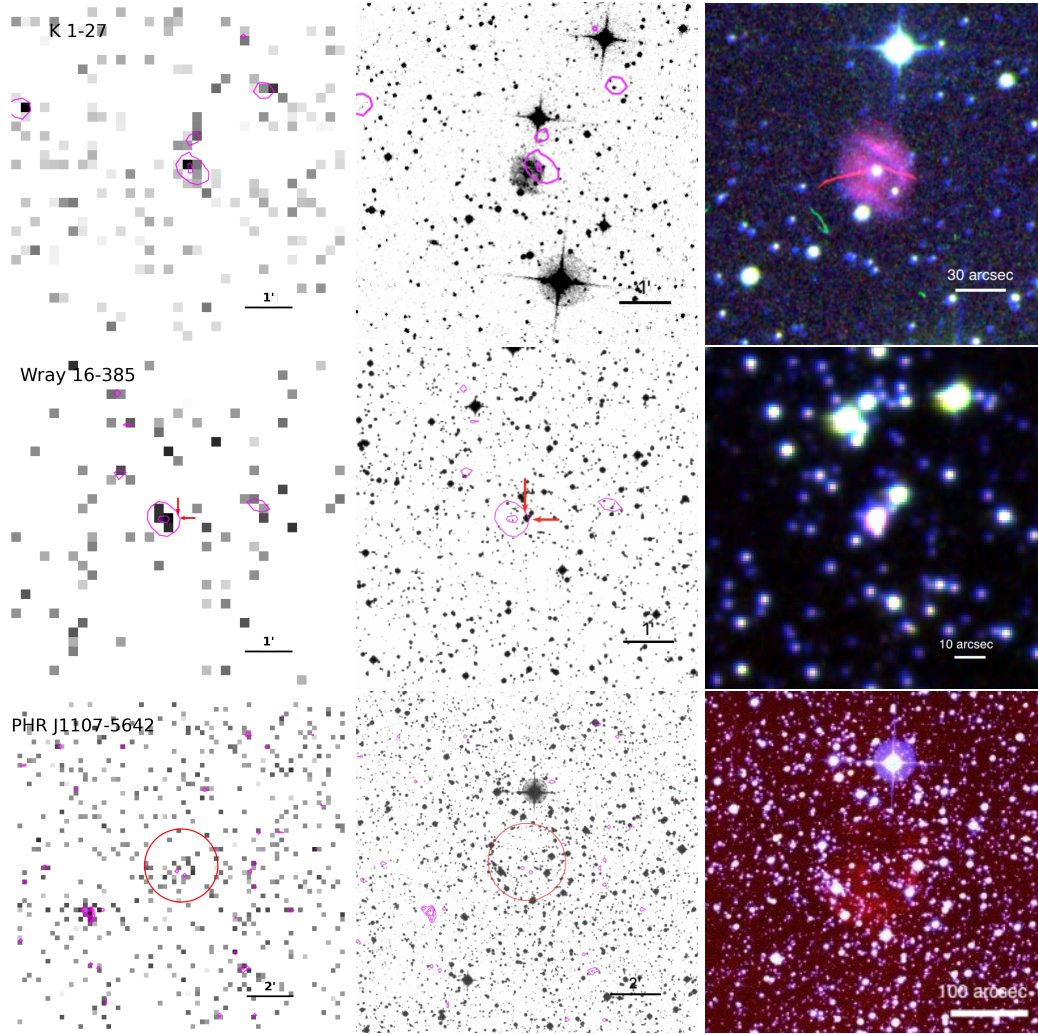


Figure 3. *eROSITA* (left) and B-band (middle) images of the three PNe with spurious eRASS1 counterparts overlaid by X-ray contours. The X-ray and B-band images have the same 7×7 arcmin field of view (PHR J1107–5642 has 14×14 arcmin). North is up, east to the left. The final image in each case is an RGB colour combination from the SHS and SuperCOSMOS sky survey photographic data, with $H\alpha$ the red channel, SR the green channel, and B_j the blue channel, all adjusted to best reveal the PN. The red arrows on the *eROSITA* and B-band images for Wray 16-385 show the location of the PN offset from the X-ray source

by M. A. Guerrero et al. (2012). The low count number and peculiarities of the X-ray emission from Abell 30 and the absorption component certainly account for this discrepancy.

3.1.3. NGC 3242, the Ghost of Jupiter Nebula

NGC 3242 is another well-known, iconic, multiple shell PN (e.g. T. Barker 1985; L. Konstantinou et al. 2025), discovered by William Herschel in 1785. It is at a distance of 1340 ± 90 pc based on its CSPN Gaia detection. Diffuse X-ray emission within its innermost shell was first detected by XMM-Newton (N. Ruiz et al. 2011). The X-ray emission is soft, with most photons with energies below 1.0 keV and very little emission at higher energies. It can be described by a thin-plasma emission model at a temperature of $\sim 2.35 \times 10^6 K$, with an observed X-ray flux of 4×10^{-4} erg cm $^{-2}$ s $^{-1}$ and an intrinsic X-ray luminosity in the 0.4-2.0 keV band of 4×10^{31} erg s $^{-1}$. In this sense, the detection of these soft X-ray photons is favored by the low extinction towards NGC 3242, with a hydrogen column density $N_H = 5 \times 10^{20}$ cm $^{-2}$ according to the logarithmic extinction coefficient of $c(H\beta) = 0.12$ derived by S. R. Pottasch & J. Bernard-Salas (2008). The diffuse X-ray emission from NGC 3242 was confirmed to be confined within its innermost shell, which can then be described as a hot bubble powered by the stellar wind, by Chandra observations

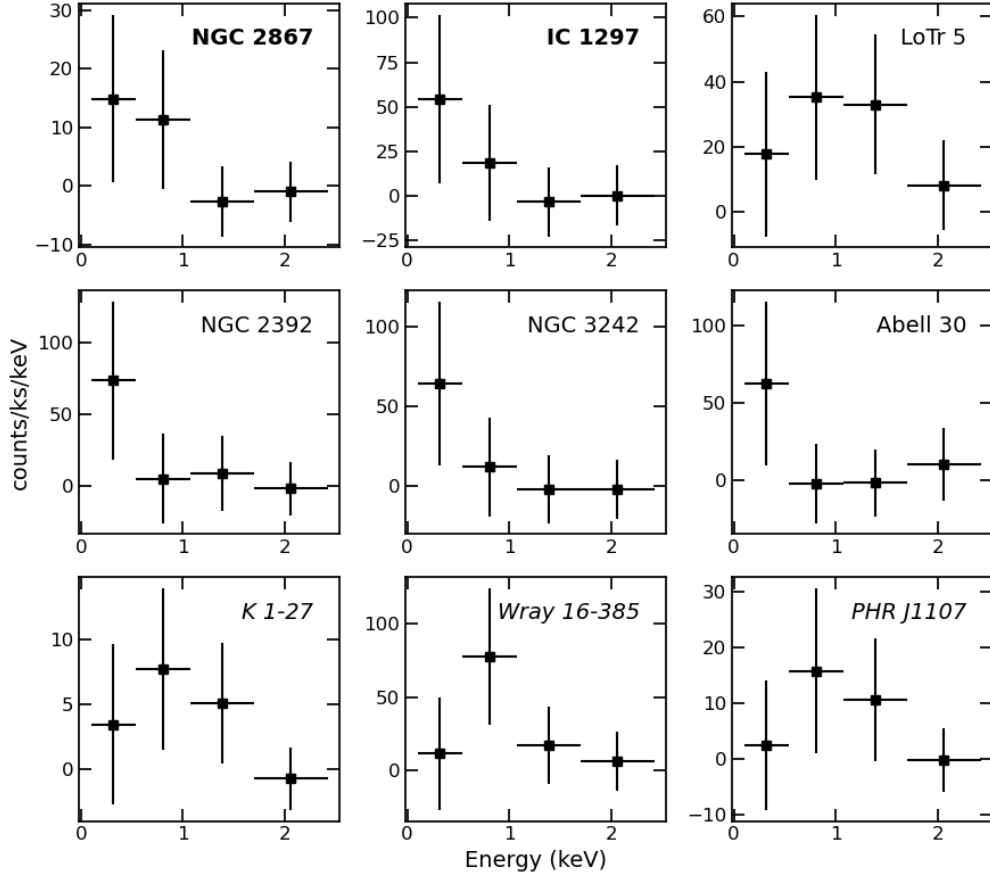


Figure 4. *eROSITA* background-subtracted spectra of the X-ray counterparts of PNe in eRASS1 with limited count number. The peak at low photon energy distributions for the 5 confirmed X-ray emitting PNe compared to the 3 rejected candidates K 1-27, Wray 16-385 and PHR J1107-5642 is clear.

with superior spatial resolution (J. H. Kastner et al. 2012). There is no detectable X-ray emission from the central star.

With a similar PSF to XMM-Newton, the X-ray emission detected by *eROSITA* perfectly matches the position of NGC 3242, with most X-ray photons enclosed within the innermost shell. The count number, $\simeq 6$, is once again insufficient for spectral analyses, but the spectral shape in Fig. 4 is consistent with the soft X-ray emission from this PN. The median energy of these events, $\simeq 0.46$ keV, and low extinction suggest a plasma temperature in the range $(1 - 2) \times 10^6$ K (Fig. 6)—v.

3.1.4. NGC 5315

NGC 5315 is another reasonably well-known, high surface brightness PN (e.g. M. Peimbert et al. 2004; S. R. Pottasch et al. 2002). Its X-ray emission was serendipitously detected in Chandra observations (ObsID 4480) that were actually targeting another PN, Hen 2-99 which ironically itself was not detected. The X-ray spectrum of NGC 5315 is consistent with emission from a hot plasma at $T_X \sim 2.5 \times 10^6$ K with enhanced Ne abundances (J. H. Kastner et al. 2008). The observed X-ray flux is $\simeq 1 \times 10^{-13}$ erg cm $^{-2}$ s $^{-1}$, for an intrinsic X-ray luminosity at the Gaia distance⁷ of 4×10^{31} erg s $^{-1}$ in the 0.3 – 2.0 keV energy band (J. H. Kastner et al. 2008) of 960 ± 190 pc. The X-ray-luminous hot bubble presents emission in the soft band with the extinction of $c(H_\beta) = 0.54$, and column density of $N_H = 2.2 \times 10^{21}$ cm $^{-2}$ (S. R. Pottasch et al. 2002).

The X-ray emission detected by *eROSITA* perfectly matches the position of NGC 5315. The count number, $\simeq 43$, is sufficient for spectral analyses (Fig. 5). The spectrum shows a prominent Ne IX line at ≈ 0.9 keV, which causes

⁷ J. H. Kastner et al. (2008) adopted a distance of 1.5 kpc, resulting in a larger estimate of the X-ray luminosity of 2.5×10^{32} erg s $^{-1}$.

the increase of the median energy of the events, $\simeq 0.62$ keV, over that of the previously discussed PNe. Adopting the same Ne and Fe abundances to be 4.3 and 0.6 times solar, respectively, derived by J. H. Kastner et al. (2008), the best-fit parameters are a hydrogen column density $N_{\text{H}} = 2.1 \times 10^{21} \text{ cm}^{-2}$, a plasma temperature of 1.9×10^6 K (see also Fig. 6) and an observed flux in the 0.1-2.0 keV range of $(1.7 \pm 0.3) \times 10^{-13} \text{ erg cm}^{-2} \text{ s}^{-1}$. The intrinsic X-ray luminosity would be $\approx 2.3 \times 10^{32} \text{ erg s}^{-1}$.

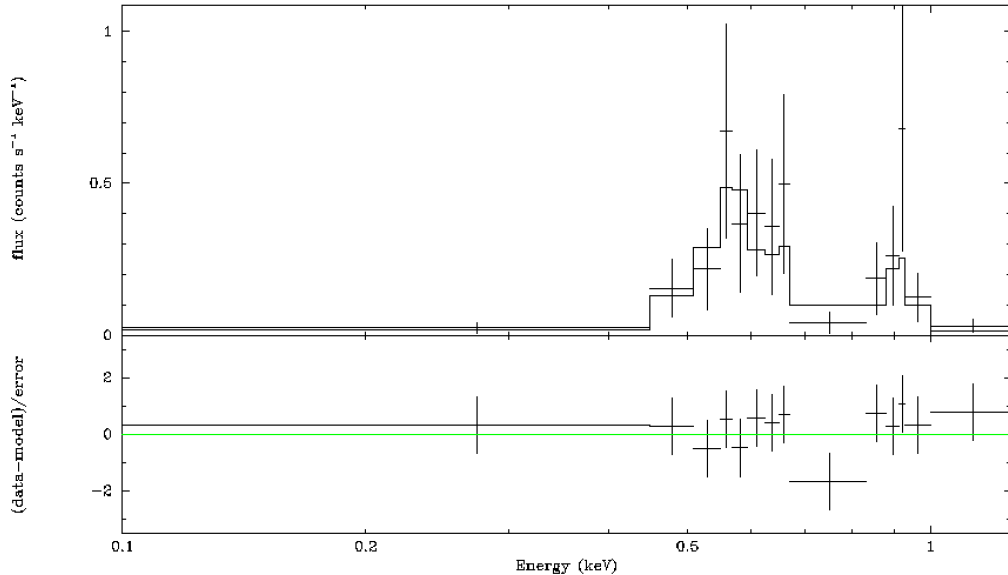


Figure 5. (top panel) *eROSITA* background-subtracted X-ray spectrum of NGC 5315 (dots) overlaid with the best-fit model (histogram). (bottom) Residuals of the best-fit model.

3.1.5. *LoTr 5*

LoTr 5 is an extended ($\sim 7' \times 8'$ in size) nebula of low surface brightness but with a bright CSPN. It was first reported detected in X-rays by ROSAT (H. C. Kreyssing et al. 1992) and has been reasonably well studied (e.g. F. Thevenin & G. Jasiewicz 1997; D. Jones et al. 2017). It has been described to have a bipolar structure oriented almost along the line of sight (M. F. Graham et al. 2004). It is located near RXJ 1256.0+2556, a fossil galaxy group of high X-ray luminosity (H. G. Khosroshahi et al. 2007). As a result, LoTr 5 was serendipitously observed by both Chandra and XMM-Newton, thus providing new, valuable X-ray data. Its low density and large angular size imply an evolved nebula, unusual for the X-ray emitting hot bubble of a PN. A thorough analysis of these X-ray data actually finds that there is no diffuse X-ray emission from a hot bubble (R. Montez et al. 2010), but it instead arises from its central star. This is the known long-period binary system IN Com (first suggested by A. Acker et al. 1985) formed by a hot, 150,000 K, CSPN and a rapidly-rotating G5 III companion⁸. Its X-ray emission can be described using a two-temperature optically-thin plasma model of 7.5×10^6 and $(26-41) \times 10^6$ K, respectively (R. Montez et al. 2010). The observed X-ray flux seemed to vary among the XMM-Newton and Chandra observations from 9×10^{-14} to $2.3 \times 10^{-13} \text{ erg cm}^{-2} \text{ s}^{-1}$, respectively, indicating possible intense activity. Accordingly, the intrinsic X-ray luminosity at the Gaia distance of 455 ± 10 pc ranges from 2.2×10^{30} to $4.4 \times 10^{30} \text{ erg s}^{-1}$, respectively.

The new *eROSITA* detection confirms the association of the X-ray emission with the central star of LoTr 5. The spectral shape is quite flat and indicates a hard spectrum, with a median energy of 0.73 keV, higher than the typical value associated with hot bubbles in PNe (Fig. 6), but consistent with the hard X-ray emission from the G5 III component of IN Com. The background-subtracted spectrum has 15 counts. Adopting the two thin thermal plasma

⁸ The system has been proposed to include an additional tertiary component to the giant component (G. Jasiewicz et al. 1987; A. Aller et al. 2018), which might be responsible for its unusual rapid rotation.

models, the plasma temperatures are simulated as 0.034 and 2.5 keV, respectively (with a reduced χ^2 of 1.23). The flux is estimated to be 1.3×10^{-13} erg cm $^{-2}$ s $^{-1}$. The X-ray emission level matches those of previous archival spectral analyses (R. Montez et al. 2010).

3.2. New X-ray-emitting Galactic PNe in the *eROSITA* *eRASS1*

The inspection of the X-ray and optical images of possible *eRASS1* counterparts of Galactic PNe has resulted in the discovery of X-ray emission from NGC 2867 and IC 1297. These had not been targeted before by Chandra or XMM-Newton and are thus two new additions to the list of known X-ray-emitting PNe described below.

3.2.1. NGC 2867

NGC 2867 (a.k.a. Caldwell 90) is a prominent, high surface brightness PN with a faint, outer halo (e.g. L. H. Aller et al. 1981) discovered by John Herschel in 1834. Its central star has been classified as a [WC3] with a terminal wind velocity $\simeq 2000$ km s $^{-1}$ and the mass loss rate is estimated as $\simeq 3 \times 10^{-8}$ M $_{\odot}$ yr $^{-1}$ (G. R. Keller et al. 2014).

The location of the X-ray emission matches the optical nebula. The number of detected X-ray photons, 8.7 ± 3.3 , is insufficient for a detailed spectral analysis, but we note that its *eROSITA* background-subtracted spectrum in Fig. 4 is relatively similar to that of NGC 3242 while softer than that of NGC 5315. Its median energy is ~ 0.55 keV, which, according to its column density, is indicative of a plasma temperature $\simeq 2 \times 10^6$ K (Fig. 6). We thus propose it to be associated with a hot bubble.

3.2.2. IC 1297

IC 1297 is a high surface brightness but little studied bipolar PN with a clear CSPN (L. H. Aller et al. 1986). Its morphology is actually reminiscent to that of NGC 6543. Its CSPN is also classified as [WR] with spectral type [WO3] (A. Acker & C. Neiner 2003).

Just as for NGC 2867, the location of the X-ray emission matches the optical nebula.

The detected X-ray photons, 7.3 ± 4.0 , are once again insufficient for detailed spectral analyses, but it is also noted that the background-subtracted spectrum of IC 1297 in Fig. 4 is almost identical to that of NGC 3242. Furthermore, the median energy of these photons, ~ 0.44 keV, in conjunction with the hydrogen column density towards IC 1297, places it close to the locus of X-ray PNe with hot bubbles at a temperature $\simeq 1 \times 10^6$ K (Fig. 6). In view of these properties, we also propose it to be associated with a hot bubble.

3.3. Galactic PNe with spurious *eROSITA* *eRASS1* counterparts

The cross-correlation of the *eRASS1* catalogue and HASH resulted in three additional potential matches, K 1-27 (previously identified as an X-ray emitter), Wray 16-385, and PHR J1107–5642. For various reasons, briefly outlined below, these are considered to be unreliable matches. Firstly, they exhibit none of the same optical nebula characteristics compared to the extant previously confirmed PNe that are also X-ray emitters such as having high surface brightness and prominent CSPN. Secondly, for both K 1-27 and Wray 16-385, there is a small but clear misalignment between the optical coordinate of the centre of the PN and the X-ray coordinate of its possible *eRASS1* counterpart, which are $4.7\text{-}\sigma$ and $6.0\text{-}\sigma$ apart, respectively. For the third case the detection of X-ray emission from PHR J1107–5642 is also highly dubious. Two factors are problematic in this case. These are the large angular size (188 arcsec in diameter) and optically faintness of the PN. These would be unprecedented for an X-ray emitting PN compared to all previously confirmed X-ray emitting PNe so we consider that the cross-correlation positional co-incidence is due to a background source in close angular projection to the PN centroid.

The spectral properties of the putative X-ray counterparts of K 1-27 and Wray 16-385 have median energies of 1.0 and 0.65 keV, respectively. The *eROSITA* median energy of K 1-27 is higher than the typical value for PNe in Tables 1 and 2, making it a very unlikely X-ray value for a PN. For Wray 16-385, its *eROSITA* median energy is also relatively high, although not completely incompatible with PNe or one with coronal emission from a companion of its central star. The X-ray spectra of these three sources in Fig. 4 clearly differ from those of confirmed X-ray-emitting PNe.

The X-ray history of K 1-27 is short, with limited previous literature available, but interesting to discuss. T. Rauch et al. (1994b) obtained a pointed ROSAT PSPC observation and claimed detection of X-ray emission from its central star. M. Guerrero et al. (2000) examined these same observations and cast doubt on the association between the X-ray emission and K 1-27. This was because the X-ray emission spectral shape was not the typical of PNe while the positional match was not considered sufficiently robust. These doubts are now confirmed here with our *eROSITA*

Table 4. X-ray-emitting Galactic PNe observed by eROSITA-DE in eRASS1.

PN Name	d (pc)	eRASS1 count rate (s ⁻¹)	Satellite	f_X (erg cm ⁻² s ⁻¹)	T_X (10 ⁶ K)	L_X (erg s ⁻¹)	X-ray References
Detected by eROSITA							
Abell 30	2210 ± 160	0.071 ± 0.036	XMM & Chandra	2.8×10^{-14}	0.79	1.3×10^{31}	1
IC 1297	4400 ± 1100	0.091 ± 0.038	eROSITA	4.6×10^{-14}	...	$> 1 \times 10^{32}$	This paper
LoTr 5	455 ± 10	0.136 ± 0.035	XMM, Chandra	$(9 - 23) \times 10^{-14}$	7.5, 26 - 41	$(2.4 - 4.4) \times 10^{30}$	2
NGC 2392	1830 ± 90	0.094 ± 0.038	XMM, Chandra	6×10^{-14}	2	4.1×10^{31}	3, 4
NGC 2867	2900 ± 500	0.032 ± 0.012	eROSITA	1.6×10^{-14}	...	$> 2 \times 10^{31}$	This paper
NGC 3242	1340 ± 90	0.083 ± 0.036	XMM, Chandra	4×10^{-14}	2.4	4×10^{31}	5
NGC 5315	960 ± 190	0.264 ± 0.043	Chandra	1.0×10^{-13}	2.6	4×10^{31}	6
Undetected by eROSITA							
DS 1	815 ± 21	0.011 ± 0.005	Chandra	9.5×10^{-15}	3.1, 14.5	1×10^{30}	2
IC 418	1360 ± 50	0.000 ± 0.004	Chandra	2.5×10^{-15}	3.0	2.7×10^{31}	4
Hb 5	3200:	0.040 ± 0.009	XMM & Chandra	7.9×10^{-15}	2.4 - 3.7	1.5×10^{32}	7
HbDs 1	746 ± 23	0.014 ± 0.006	Chandra	5×10^{-15}	2.1	4.7×10^{29}	8
LO 16	1820 ± 150	0.010 ± 0.009	Chandra	8.3×10^{-16}	15.9	5.3×10^{29}	8
NGC 1360	400 ± 50	0.018 ± 0.004	Chandra	1.4×10^{-14}	1.4	2.8×10^{29}	8
NGC 2371-2	1720 ± 140	0.040 ± 0.005	Chandra	9
NGC 4361	1040 ± 50	0.023 ± 0.009	Chandra	1.7×10^{-14}	0.67	2.8×10^{30}	8
NGC 6153	1390 ± 90	0.015 ± 0.005	Chandra	9
NGC 6337	1680 ± 110	0.019 ± 0.009	Chandra	7.0×10^{-15}	8.3 - 14.4	1.8×10^{31}	8
Sp 1	1393 ± 32	0.007 ± 0.004	Chandra	1.3×10^{-15}	0.6 - 3.2	1.2×10^{30}	8

(1) M. A. Guerrero et al. (2012); (2) R. Montez et al. (2010); (3) M. A. Guerrero et al. (2005); (4) N. Ruiz et al. (2013);
(5) N. Ruiz et al. (2011); (6) J. H. Kastner et al. (2008); (7) R. Montez et al. (2009); (8) R. Montez et al. (2015);
(9) M. Freeman et al. (2014)

eRASS assessments leading to the conclusion that the X-ray emission is most likely a background source unrelated to K 1-27.

4. DISCUSSION

Below we provide a brief summary of the main findings from this *eROSITA* study of PNe.

4.1. Frequency of Occurrence of X-ray-emitting PNe and Typical X-ray Flux

The cross-correlation between all 1430 HASH ‘True’ Galactic PNe that fall within the accessible *eROSITA*-DE eRASS1 source catalogue footprint ($179.94423568^\circ \leq l \leq 359.94423568^\circ$), resulted in a list of 10 PNe with possible eRASS1 candidate counterparts. Based on this work only seven can now be considered bona-fide eRASS1 PNe (Tabs. 1 and 2). This implies that of True HASH PNe only $\simeq 0.5\%$, are detected in the eRASS1. Their properties are listed in Table 4. The 11 true Galactic PNe previously confirmed as X-ray-emitters and falling in the available eRASS1 footprint but that are not detected by *eRosita* are also listed in Table 4 together with their properties. Unsurprisingly all of them have X-ray fluxes below the nominal all-sky eRASS1 flux sensitivity limit of 5×10^{-14} erg cm⁻² s⁻¹. The eRASS1 PNe Abell 30, NGC 3242, and most likely NGC 2867 also nominally fall below this base-level sensitivity limit, However, this varies across the sky, improving at high ecliptic latitudes which is the situation for most of these cases. It is certainly better for NGC 2867, the faintest eRASS1 PN, which has an exposure time of 269 seconds, well above the average. The comparison between X-ray PNe detected and undetected in eRASS1 in Table 4 can be used to set an average upper limit for the X-ray flux of the 1430 True PNe in the Western, German region of eROSITA coverage. Comparing the detected Abell 30 and undetected NGC 4361, a threshold $\approx 2 \times 10^{-14}$ erg cm⁻² s⁻¹ can be determined. We can conclude that most (99.5%) PNe in the Western, German footprint of eROSITA have X-ray fluxes below this threshold. Their low X-ray flux can be expected to be the result of a combination of distance, extinction, evolutionary status and inherent PN characteristics.

4.2. The eRASS1 X-ray PNe

The eRASS1 catalogue includes the detection of five already known X-ray emitting PNe and two new detections. The nature of the five already known X-ray PNe detected by *eRosita* is varied: Abell 30 is an extremely soft X-ray source, while NGC 2392, NGC 3242, and NGC 5135 are hot bubbles of diffuse emission with varying plasma properties and extinction column densities. LoTr 5 an apparently more evolved PN, is an X-ray point-source emitter arising from the interaction of the CSPN with a G-type companion. In general the spectral properties of X-ray PNe are different. This is also the case of the particular PNe detected by *eRosita*, as revealed in Figs. 4 and 6. Therefore a unique conversion factor from count rate to X-ray flux cannot be derived. To overcome this issue, the X-ray flux of these PNe,

as derived from high quality Chandra or XMM-Newton spectra, are plotted in Figure 7 against the observed eRASS1 EML1 band count rate. The red solid line shows the best linear-fit. The corresponding conversion factor from count rate to X-ray flux for PNe (red line in the plot) is found to be $(5.1 \pm 1.3) \times 10^{-13} \text{ erg cm}^{-2} \text{ s}^{-1}$.

No spectral fit is possible to the count-starved *eROSITA* spectra of the new X-ray PNe IC 1297 and NGC 2867. Their optical morphologies (right panels in Fig. 2) and X-ray spectral properties (median photon energy in Tab. 4 and Fig. 6 and X-ray spectra in Fig. 4) are otherwise highly indicative of thermal plasma emission from hot bubbles. Using the conversion factor from eRASS1 EML1 count rate to X-ray flux, we derive X-ray fluxes of $(4.6 \pm 2.2) \times 10^{-14}$ and $(1.6 \pm 0.7) \times 10^{-14} \text{ erg cm}^{-2} \text{ s}^{-1}$ for IC 1297 and NGC 2867, respectively. The intrinsic X-ray flux cannot be derived, but lower limits can be set from their observed X-ray fluxes and distances (see Tab. 4).

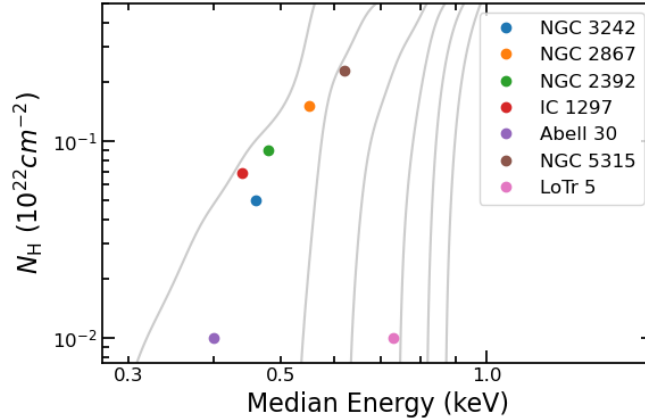


Figure 6. Median energy and column density plane for the eRASS1 X-ray PNe. Gray lines are for plasma temperatures of 1, 2, 3, 5, 8, and 10 MK increasing from the left to the right.

Both IC 1297 and NGC 2867 harbour [WR] CSPNe of spectral type [WO3] and [WC2], respectively. This is relevant because it has been recognized in the past the existence of two different families of hot bubbles, those produced by H-rich CSPNe and those associated with [WR] CSPNe, with the more powerful stellar winds of the latter result in higher X-ray luminous PNe (J. H. Kastner et al. 2000; M. Freeman et al. 2014; J. A. Toalá et al. 2019). The X-ray luminosity of IC 1297 is certainly high, typical of PNe with [WR] central stars. That of NGC 2867, which is absorbed by a large column density, $\approx 2 \times 10^{21} \text{ cm}^{-2}$, can also be expected to be high. These results further strengthen the X-ray expectations for PNe hosting [WR] central stars.

5. CONCLUSIONS AND EXPECTATIONS FOR NEW X-RAY MISSIONS INCLUDING THE EINSTEIN PROBE

The *eROSITA* eRASS1 catalogue has provided, for the first time, a survey of (half) the sky in X-rays at the sensitivity required to detect the soft and faint X-ray emission from hot bubbles of PNe and that of their CSPNe. Although 1430 True PNe from HASH with Galactic longitude $\gtrsim 180^\circ$ are included in the footprint of eRASS1, only seven are detected, implying a low ($\approx 0.5\%$) success rate, i.e., only one out of 200 PNe is found to exhibit X-ray emission at levels of a few times $10^{-14} \text{ erg cm}^{-2} \text{ s}^{-1}$ that *eROSITA* is sensitive to. Future X-ray missions targeting PNe must have higher sensitivity to be capable of producing useful detections of a more statistically significant sample. Future *eROSITA* eRASS data releases and the availability of the Russian hemisphere *eRosita* data would be valuable to add further detections, but these questions are unfeasible for the time being.

The new X-ray detections presented in this paper, namely IC 1297 and NGC 2867, both host [WR]-type CSPNe, confirming their superior levels of X-ray emission compared to PNe with H-rich CSPNe. Pointed observations of these two PNe would be very useful to assess the properties of their X-ray-emitting gas and compare them with the nebular and stellar wind properties. We have begun an observing program with the Chinese Einstein Probe (EP) "lobster eye" X-ray telescope (W. Yuan et al. 2015, 2018, 2022) to follow up some of the X-ray emitting PNe here but also others we have identified that have various common observational and physical characteristics that make them likely X-ray emitting PNe. The EP Wide-field X-ray Telescope features a 3600 sq. degree field of view, giving it the largest grasp among existing soft X-ray focusing telescopes. With an effective area of 600 cm^2 , decent angular resolution of $\leq 30''$

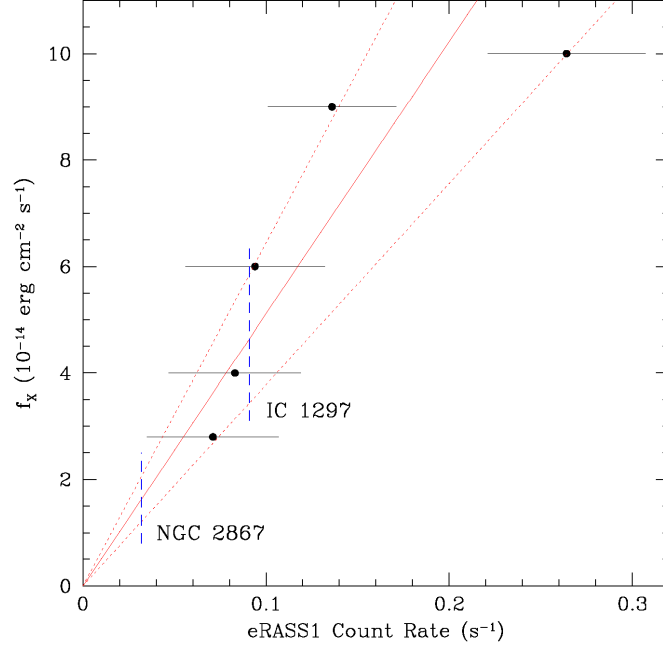


Figure 7. eROSITA count rate in the EML1 energy band and X-ray flux of the X-ray-emitting PNe. The red solid line corresponds to the best-linear fit, whereas the red dotted lines consider $1\text{-}\sigma$ dispersion. The count rates of IC 1297 and NGC 2867 are marked by vertical dashed blue lines.

(HPD), and a quick response time, the EP is among the most powerful X-ray telescopes. The strength of EP is in its rapid follow-up capability for observing transient X-ray sources, and it also works well for soft X-ray sources.

The EP has similar base level performance in terms of spatial resolution/effective area to eROSITA, but unlike eROSITA, which operated in survey mode, the EP is an X-ray observatory that can make pointed and therefore deeper integrations up to tens of kilo-seconds if deemed necessary, reaching a sensitivity $\simeq 10^{-14}$ erg cm $^{-2}$ s $^{-1}$ in a 10 ks exposure (J. Zhang et al. 2022). At the same exposure level, Chandra ASIC and XMM-Newton have flux limits of 4×10^{-15} erg cm $^{-2}$ s $^{-1}$ and 8.4×10^{-14} erg cm $^{-2}$ s $^{-1}$ respectively.

These new telescopes would enhance the detection of GRBs and supernovae, offering continuous power for exploring the universe.

6. ACKNOWLEDGEMENTS

We are grateful to the anonymous referee whose suggestions and feedback have improved the paper. HY thanks QAP, HKU and the Laboratory for Space Research for the provision of a PhD scholarship. MAG acknowledges financial support from grants CEX2021-001131-S funded by MCIN/AEI/10.13039/501100011033 and PID2022-142925NB-I00 from the Spanish Ministerio de Ciencia, Innovación y Universidades (MCIU) co-funded with FEDER funds. QAP thanks the Hong Kong Research Grants Council for GRF research grants 17326116, 17300417 and 17304520. We made use of NASA’s Astrophysics Data System; The German eROSITA Consortium Data Release 1 (DR1); the SIMBAD database operated at CDS, Strasbourg, France; Astropy, a community-developed core Python package for Astronomy (T. A. Collaboration et al. 2022); Javalambre Photometric Local Universe Survey; HASH, an online database at the Laboratory for Space Research at HKU federates available multi-wavelength imaging, spectroscopic; and other data for all known Galactic PNe and is available at: <http://www.hashpn.space>. This work is based on data from eROSITA, the soft X-ray instrument aboard SRG, a joint Russian-German science mission supported by the Russian Space Agency (Roskosmos), in the interests of the Russian Academy of Sciences represented by its Space Research Institute (IKI), and the Deutsches Zentrum für Luft- und Raumfahrt (DLR). The SRG spacecraft was built by Lavochkin Association (NPOL) and its subcontractors, and is operated by NPOL with support from the Max Planck Institute for Extraterrestrial Physics (MPE). The development and construction of the eROSITA X-ray instrument was led by MPE, with contributions from the Dr. Karl Remeis Observatory Bamberg & ECAP (FAU Erlangen-Nuernberg), the University of Hamburg Observatory, the Leibniz Institute for Astrophysics Potsdam (AIP), and the Institute for

Astronomy and Astrophysics of the University of Tübingen, with the support of DLR and the Max Planck Society. The Argelander Institute for Astronomy of the University of Bonn and the Ludwig Maximilians Universität Munich also participated in the science preparation for eROSITA.

REFERENCES

- Acker, A., Jasniewicz, G., & Gleizes, F. 1985, *A&A*, 151, L13
- Acker, A., & Neiner, C. 2003, *A&A*, 403, 659, doi: [10.1051/0004-6361:20030391](https://doi.org/10.1051/0004-6361:20030391)
- Aller, A., Lillo-Box, J., Vučković, M., et al. 2018, *MNRAS*, 476, 1140, doi: [10.1093/mnras/sty174](https://doi.org/10.1093/mnras/sty174)
- Aller, L. H., Keyes, C. D., & Feibelman, W. A. 1986, *ApJ*, 311, 930, doi: [10.1086/164830](https://doi.org/10.1086/164830)
- Aller, L. H., Keyes, C. D., Ross, J. E., & Omara, B. J. 1981, *MNRAS*, 197, 647, doi: [10.1093/mnras/197.3.647](https://doi.org/10.1093/mnras/197.3.647)
- Barker, T. 1985, *ApJ*, 294, 193, doi: [10.1086/163286](https://doi.org/10.1086/163286)
- Boller, T., Freyberg, M. J., Trümper, J., et al. 2016, *A&A*, 588, A103, doi: [10.1051/0004-6361/201525648](https://doi.org/10.1051/0004-6361/201525648)
- Cenarro, A. J., Moles, M., Cristóbal-Hornillos, D., et al. 2019, *A&A*, 622, A176, doi: [10.1051/0004-6361/201833036](https://doi.org/10.1051/0004-6361/201833036)
- Chu, Y., Chang, T. H., & Conway, G. M. 1997, *The Astrophysical Journal*, 482, 891–896, doi: [10.1086/304196](https://doi.org/10.1086/304196)
- Chu, Y.-H., & Ho, C.-H. 1995, *The Astrophysical Journal*, 448, doi: [10.1086/309612](https://doi.org/10.1086/309612)
- Collaboration, T. A., Price-Whelan, A. M., Lim, P. L., et al. 2022, *The Astrophysical Journal*, 935, 167, doi: [10.3847/1538-4357/ac7c74](https://doi.org/10.3847/1538-4357/ac7c74)
- de Korte, P. A. J., Claas, J. J., Jansen, F. A., & McKechnie, S. P. 1985, *Advances in Space Research*, 5, 57, doi: [10.1016/0273-1177\(85\)90450-8](https://doi.org/10.1016/0273-1177(85)90450-8)
- Freeman, M., Montez, Jr., R., Kastner, J. H., et al. 2014, *ApJ*, 794, 99, doi: [10.1088/0004-637X/794/2/99](https://doi.org/10.1088/0004-637X/794/2/99)
- García-Díaz, M. T., López, J. A., Steffen, W., & Richer, M. G. 2012, *ApJ*, 761, 172, doi: [10.1088/0004-637X/761/2/172](https://doi.org/10.1088/0004-637X/761/2/172)
- Giesekeing, F., Becker, I., & Solf, J. 1985, *ApJL*, 295, L17, doi: [10.1086/184529](https://doi.org/10.1086/184529)
- Graham, M. F., Meaburn, J., López, J. A., Harman, D. J., & Holloway, A. J. 2004, *MNRAS*, 347, 1370, doi: [10.1111/j.1365-2966.2004.07342.x](https://doi.org/10.1111/j.1365-2966.2004.07342.x)
- Guerrero, M., Chu, Y., & Gruendl, R. 2000, *The Astrophysical Journal Supplement Series*, 129, 295–313, doi: [10.1086/313415](https://doi.org/10.1086/313415)
- Guerrero, M. A., Chu, Y.-H., & Gruendl, R. A. 2000, *ApJS*, 129, 295, doi: [10.1086/313415](https://doi.org/10.1086/313415)
- Guerrero, M. A., Chu, Y. H., Gruendl, R. A., & Meixner, M. 2005, *A&A*, 430, L69, doi: [10.1051/0004-6361:200400131](https://doi.org/10.1051/0004-6361:200400131)
- Guerrero, M. A., Chu, Y.-H., Gruendl, R. A., & Meixner, M. 2005, *A&A*, 430, L69–L72, doi: [10.1051/0004-6361:200400131](https://doi.org/10.1051/0004-6361:200400131)
- Guerrero, M. A., Toalá, J. A., & Chu, Y.-H. 2019, *The Astrophysical Journal*, 884, 134, doi: [10.3847/1538-4357/ab4256](https://doi.org/10.3847/1538-4357/ab4256)
- Guerrero, M. A., Ruiz, N., Hamann, W.-R., et al. 2012, *The Astrophysical Journal*, 755, 129, doi: [10.1088/0004-637x/755/2/129](https://doi.org/10.1088/0004-637x/755/2/129)
- Jacoby, G. H., & Ford, H. C. 1983, *ApJ*, 266, 298, doi: [10.1086/160779](https://doi.org/10.1086/160779)
- Jacoby, G. H., Hillwig, T. C., & Jones, D. 2020, *MNRAS*, 498, L114, doi: [10.1093/mnrasl/slaa138](https://doi.org/10.1093/mnrasl/slaa138)
- Jasniewicz, G., Duquenois, A., & Acker, A. 1987, *A&A*, 180, 145
- Jones, D., Van Winckel, H., Aller, A., Exter, K., & De Marco, O. 2017, *A&A*, 600, L9, doi: [10.1051/0004-6361/201730700](https://doi.org/10.1051/0004-6361/201730700)
- Kastner, J. H., Montez, Jr, R., Balick, B., & De Marco, O. 2008, *The Astrophysical Journal*, 672, 957, doi: [10.1086/523890](https://doi.org/10.1086/523890)
- Kastner, J. H., Soker, N., Vrtillek, S. D., & Dgani, R. 2000, *ApJL*, 545, L57, doi: [10.1086/317335](https://doi.org/10.1086/317335)
- Kastner, J. H., Montez, R., Balick, B., et al. 2012, *The Astronomical Journal*, 144, 58, doi: [10.1088/0004-6256/144/2/58](https://doi.org/10.1088/0004-6256/144/2/58)
- Keller, G. R., Bianchi, L., & Maciel, W. J. 2014, *MNRAS*, 442, 1379, doi: [10.1093/mnras/stu878](https://doi.org/10.1093/mnras/stu878)
- Khosroshahi, H. G., Ponman, T. J., & Jones, L. R. 2007, *MNRAS*, 377, 595, doi: [10.1111/j.1365-2966.2007.11591.x](https://doi.org/10.1111/j.1365-2966.2007.11591.x)
- Konstantinou, L., Akas, S., Garcia-Rojas, J., et al. 2025, *A&A*, 697, A227, doi: [10.1051/0004-6361/202453635](https://doi.org/10.1051/0004-6361/202453635)
- Kreysing, H. C., Diesch, C., Zweigle, J., et al. 1992, *A&A*, 264, 623
- Kwok, S., Purton, C. R., & Fitzgerald, P. M. 1978, *ApJL*, 219, L125, doi: [10.1086/182621](https://doi.org/10.1086/182621)
- Le Dû, P., Mulato, L., Parker, Q. A., et al. 2022, *A&A*, 666, A152, doi: [10.1051/0004-6361/202243393](https://doi.org/10.1051/0004-6361/202243393)
- Lucy, L. B., & White, R. L. 1980, *ApJ*, 241, 300, doi: [10.1086/158342](https://doi.org/10.1086/158342)
- Merloni, A., Lamer, G., Liu, T., et al. 2024, *A&A*, 682, A34, doi: [10.1051/0004-6361/202347165](https://doi.org/10.1051/0004-6361/202347165)
- Miszalski, B., Manick, R., Van Winckel, H., & Escorza, A. 2019, doi: [10.48550/ARXIV.1903.07264](https://doi.org/10.48550/ARXIV.1903.07264)

- Miszalski, B., Manick, R., Van Winckel, H., & Escorza, A. 2019, *PASA*, 36, e018, doi: [10.1017/pasa.2019.11](https://doi.org/10.1017/pasa.2019.11)
- Montez, Jr., R., De Marco, O., Kastner, J. H., & Chu, Y.-H. 2010, *ApJ*, 721, 1820, doi: [10.1088/0004-637X/721/2/1820](https://doi.org/10.1088/0004-637X/721/2/1820)
- Montez, Jr., R., Kastner, J. H., Balick, B., & Frank, A. 2009, *ApJ*, 694, 1481, doi: [10.1088/0004-637X/694/2/1481](https://doi.org/10.1088/0004-637X/694/2/1481)
- Montez, Jr., R., Kastner, J. H., Balick, B., et al. 2015, *ApJ*, 800, 8, doi: [10.1088/0004-637X/800/1/8](https://doi.org/10.1088/0004-637X/800/1/8)
- Parker, Q. A. 2022, *Frontiers in Astronomy and Space Sciences*, 9, 895287, doi: [10.3389/fspas.2022.895287](https://doi.org/10.3389/fspas.2022.895287)
- Parker, Q. A., Bojčić, I. S., & Frew, D. J. 2016a, in *Journal of Physics Conference Series*, Vol. 728, *Journal of Physics Conference Series (IOP)*, 032008, doi: [10.1088/1742-6596/728/3/032008](https://doi.org/10.1088/1742-6596/728/3/032008)
- Parker, Q. A., Bojčić, I. S., & Frew, D. J. 2016b, in *Journal of Physics Conference Series*, Vol. 728, *Journal of Physics Conference Series (IOP)*, 032008, doi: [10.1088/1742-6596/728/3/032008](https://doi.org/10.1088/1742-6596/728/3/032008)
- Parker, Q. A., Phillipps, S., Pierce, M. J., et al. 2005, *MNRAS*, 362, 689, doi: [10.1111/j.1365-2966.2005.09350.x](https://doi.org/10.1111/j.1365-2966.2005.09350.x)
- Parker, Q. A., Acker, A., Frew, D. J., et al. 2006, *MNRAS*, 373, 79, doi: [10.1111/j.1365-2966.2006.10950.x](https://doi.org/10.1111/j.1365-2966.2006.10950.x)
- Peimbert, M., Peimbert, A., Ruiz, M. T., & Esteban, C. 2004, *ApJS*, 150, 431, doi: [10.1086/381090](https://doi.org/10.1086/381090)
- Pottasch, S. R., Beintema, D. A., Bernard Salas, J., Koornneef, J., & Feibelman, W. A. 2002, *A&A*, 393, 285, doi: [10.1051/0004-6361:20020986](https://doi.org/10.1051/0004-6361:20020986)
- Pottasch, S. R., Beintema, D. A., Bernard Salas, J., Koornneef, J., & Feibelman, W. A. 2002, *A&A*, 393, 285–294, doi: [10.1051/0004-6361:20020986](https://doi.org/10.1051/0004-6361:20020986)
- Pottasch, S. R., & Bernard-Salas, J. 2008, *A&A*, 490, 715–724, doi: [10.1051/0004-6361:200810721](https://doi.org/10.1051/0004-6361:200810721)
- Predehl, P., Andritschke, R., Arefiev, V., et al. 2021, *A&A*, 647, A1, doi: [10.1051/0004-6361/202039313](https://doi.org/10.1051/0004-6361/202039313)
- Rauch, T., Koeppen, J., & Werner, K. 1994a, *A&A*, 286, 543
- Rauch, T., Koeppen, J., & Werner, K. 1994b, *A&A*, 286, 543
- Ruiz, N., Chu, Y.-H., Gruendl, R. A., et al. 2013, *The Astrophysical Journal*, 767, 35, doi: [10.1088/0004-637X/767/1/35](https://doi.org/10.1088/0004-637X/767/1/35)
- Ruiz, N., Guerrero, M. A., Chu, Y.-H., & Gruendl, R. A. 2011, *The Astronomical Journal*, 142, 91, doi: [10.1088/0004-6256/142/3/91](https://doi.org/10.1088/0004-6256/142/3/91)
- Thevenin, F., & Jasniewicz, G. 1997, *A&A*, 320, 913
- Toalá, J. A., & Arthur, S. J. 2016, *MNRAS*, 463, 4438, doi: [10.1093/mnras/stw2307](https://doi.org/10.1093/mnras/stw2307)
- Toalá, J. A., Montez, Jr., R., & Karovska, M. 2019, *ApJ*, 886, 30, doi: [10.3847/1538-4357/ab498e](https://doi.org/10.3847/1538-4357/ab498e)
- Weaver, R., McCray, R., Castor, J., Shapiro, P., & Moore, R. 1977, *ApJ*, 218, 377, doi: [10.1086/155692](https://doi.org/10.1086/155692)
- Wesson, R., Jones, D., García-Rojas, J., Boffin, H. M. J., & Corradi, R. L. M. 2018, *MNRAS*, 480, 4589, doi: [10.1093/mnras/sty1871](https://doi.org/10.1093/mnras/sty1871)
- Wesson, R., Liu, X. W., & Barlow, M. J. 2005, *MNRAS*, 362, 424, doi: [10.1111/j.1365-2966.2005.09325.x](https://doi.org/10.1111/j.1365-2966.2005.09325.x)
- Yuan, W., Zhang, C., Chen, Y., & Ling, Z. 2022, *Handbook of X-ray and Gamma-ray Astrophysics*, 86, doi: [10.1007/978-981-16-4544-0_151-1](https://doi.org/10.1007/978-981-16-4544-0_151-1)
- Yuan, W., Zhang, C., Feng, H., et al. 2015, *arXiv e-prints*, arXiv:1506.07735, doi: [10.48550/arXiv.1506.07735](https://doi.org/10.48550/arXiv.1506.07735)
- Yuan, W., Zhang, C., Chen, Y., et al. 2018, *Scientia Sinica Physica, Mechanica & Astronomica*, 48, 039502, doi: [10.1360/SSPMA2017-00297](https://doi.org/10.1360/SSPMA2017-00297)
- Zhang, J., Qi, L., Yang, Y., et al. 2022, *Astroparticle Physics*, 137, 102668, doi: [10.1016/j.astropartphys.2021.102668](https://doi.org/10.1016/j.astropartphys.2021.102668)